ISSN 1726-5479

SENSORS & TRANSDUCERS

vol. 103
4/09

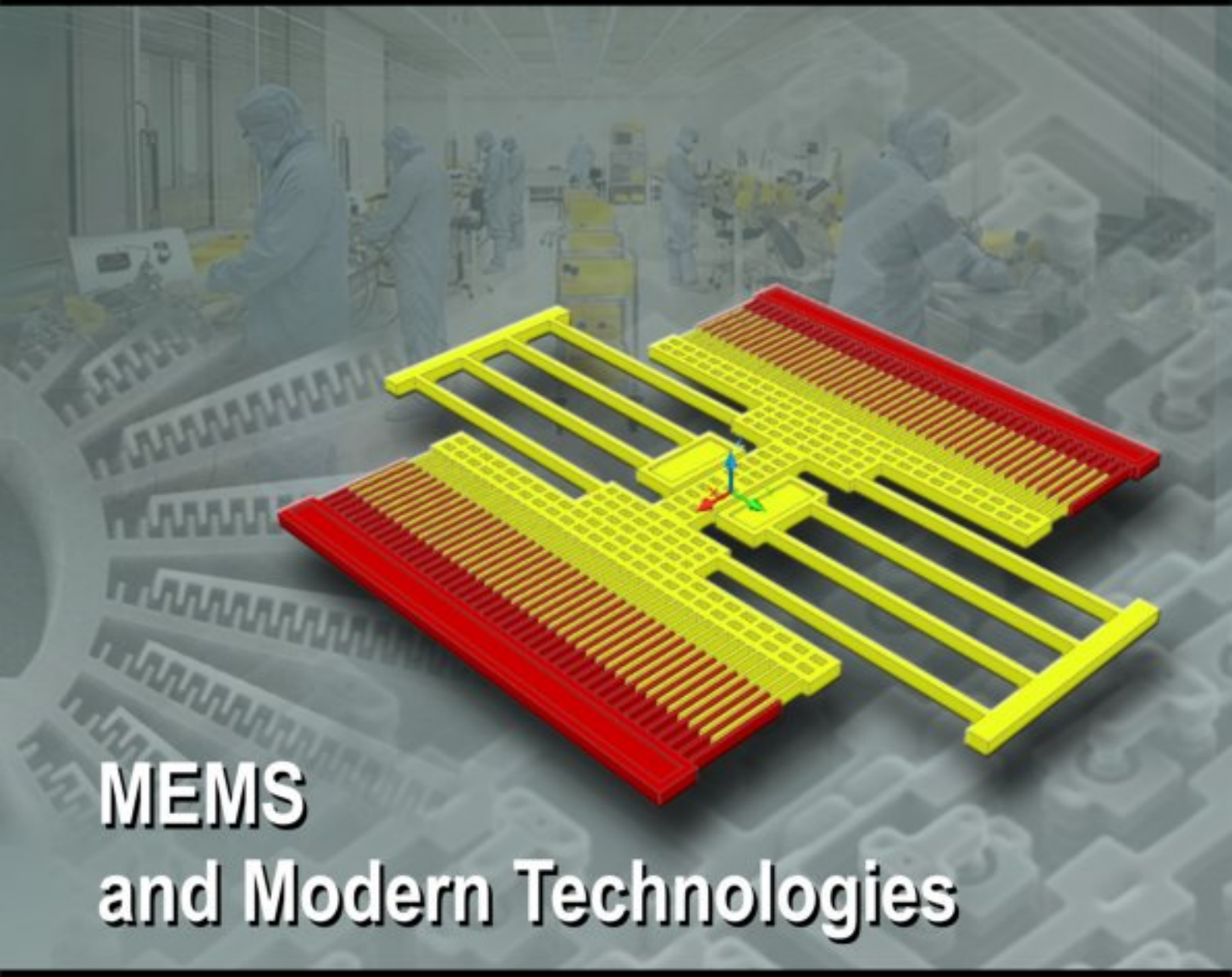

MEMS and Modern Technologies

International Frequency Sensor Association Publishing

IFSA

Sensors & Transducers

Volume 103, Issue 4
April 2009

www.sensorsportal.com

ISSN 1726-5479

Sensors & Transducers Journal (ISSN 1726-5479) is a peer review international journal published monthly online by International Frequency Sensor Association (IFSA).
Available in electronic and on CD.

Sensors & Transducers Journal

Contents

Volume 103
Issue 4
April 2009

www.sensorsportal.com

ISSN 1726-5479

Research Articles

Authors are encouraged to submit article in MS Word (doc) and Acrobat (pdf) formats by e-mail: editor@sensorsportal.com
Please visit journal's webpage with preparation instructions: http://www.sensorsportal.com/HTML/DIGEST/Submition.htm

International Frequency Sensor Association (IFSA).

Sensors & Transducers Journal, Vol. 103, Issue 4, April 2009, pp. 29-43

www.sensorsportal.com

Sensors & Transducers

ISSN 1726-5479

http://www.sensorsportal.com

Modeling of Micromachined Thermopiles Powered from the Human Body for Energy Harvesting in Wearable Devices

[1]Vladimir Leonov, [1, 2]Ziyang Wang, [1]Paolo Fiorini and [1]Chris Van Hoof

[1]Interuniversity Microelectronics Center (IMEC), Kapeldreef 75, 3001 Leuven, Belgium

[2]Catholic University Leuven, 3000 Leuven, Belgium

[1]Tel.: +32-16-288 367, fax: +32-16-281 576

E-mail: leonov@imec.be

Received: 3 February 2009 /Accepted: 20 April 2009 /Published: 27 April 2009

Abstract: The design of thermoelectric MEMS converters (power generators) suited for self-powered wearable devices is proposed and analyzed. Micromachined thermopiles are designed on top of a silicon rim and their performances are modeled for two thermoelectric materials, BiTe and polycrystalline SiGe. The advantage of the proposed design in respect to existing ones is a large output voltage combined with a relatively large generated power. The design is developed for a watch size generator and takes into account limitations of contact lithography in terms of aspect ratio and minimum feature size. Within these limitations, the output voltage is close to 1V while the output power is in excess of 1 μW for poly-SiGe based generators and close to 10 μW for BiTe based ones.

Keywords: Thermoelectric generator, Energy harvesting, MEMS, Thermopile

1. Introduction

Low power consumption of silicon-based electronics has enabled a broad variety of battery-powered handheld, wearable and implantable devices. It is expected that in the near future electronic circuits will consume less power, further shrink in dimensions, or will provide more functionalities in the same volume. Such rapid scaling down is not foreseen for batteries that become the limiting factor in development of portable electronics. Therefore, many developments are ongoing to replace batteries with higher density storage fuel-based systems such as fuel cells and microturbines. Among the

various applications demanding long-lasting power sources, wireless networks of autonomous sensors is the one of the most challenging. These networks should consist of sensors deployed in streets, houses, offices, cars, on the human body, or in remote locations that are not always accessible. Sensors in such networks measure various physical quantities and transmit their values to a central station. As the power consumption of these nodes can be relatively low, the research is ongoing on "free" sources of environmental energy and on effective ways of converting such energy into electricity. This strategy, known as energy scavenging or energy harvesting, will make the wireless sensor network autonomous, and will enable avoiding periodic changing batteries. Among the possible 'perpetual' power generators, solar cells are successful on the market for decades and their annual production rapidly grows. Nevertheless, the illumination level in buildings is frequently low, which makes solar cells much less efficient in indoor applications. The other possible energy sources for harvesting in urban environment are natural and artificial flows of air or water, vibrations, movements and thermal waste in machinery, traffic as well as the other thermal gradients available in a city. People themselves and their pets are also possible candidates for energy harvesting in wearable devices. Historically, the watch art and industry have first drawn their attention at the possibility of energy harvesting for a "perpetual" wearable device by getting the required energy from walking and other physical activities of a person. Harvesting this type of energy in watches is known for two centuries since the invention of self-winding pocket watch by Abraham-Louis Perrelet in about 1770.

Seeking for complementary power sources for modern autonomous devices, one can spot a remarkable feature of the authors and the reader: we are typically warmer than the environment. Again, as in case of mechanical energy, the natural heat flow from the human body into the ambient air was first used to power a wristwatch [1, 2]. However, watches consume very low power: only about 1 μW is required to drive modern low-power electronic watch. In contrast, much more energy, i.e., several milliwatts, is typically required for the simplest wireless sensor nodes. While targeting at autonomous operation of sensors on human beings, certain power saving steps can be effectively performed at a circuit design level, accompanied by tuning electronic components to low power consumption regimes. In addition, a duty-cycling should be applied, where possible, in particular, for the radio transmission. By doing so, wireless sensor nodes powered by wrist thermoelectric generators based on commercial thermopiles have been demonstrated [3, 4]. Their operation has shown that 50–100 μW transferred to the electronics are enough for self-powering duty-cycled wireless sensor nodes of today, so much less power will be enough for tomorrow's devices or for event-driven devices. The thermoelectric generators used in systems referred above, however, remain too costly for the market, because their closest competitors, namely, batteries and photovoltaic cells are much cheaper. The development of micromachined thermal energy harvesters for replacing commercial thermopiles would drastically decrease the system production cost thereby making feasible the mass production of low-cost devices and sensor networks powered by heat of human beings, animals and machines. This paper discusses effective designs for both the thermopile and thermoelectric generator (TEG) for application on low-grade heat sources such as a human being or other warm-blooded animals. In spite of human-oriented research, the TEGs could effectively work on other heat sources mentioned above.

2. Thermopiles for Wearable Devices: State of the Art

Two basic types of thermopiles for wearable energy harvesters currently attract the attention of the scientific community, i.e., thick-film thermopiles and micromachined thermopiles. Both approaches are promising for cooling microelectronic components and for using them in TEGs, furthermore, they can offer low-cost fabrication processes. The latter feature is even more important than the performance characteristics themselves because all the efforts are market-driven and market-oriented. While the designs for the thermopiles can significantly differ from each other depending on related application, i.e., for cooling or for power generation, the technology could be very similar.

Ni-Cu thermopiles on waved polyimide tape placed in between two graphite plates have been described in [5, 6]. However, an output voltage of less than 1mV (on a matched load) and an output power of half nanowatt have been practically measured on human body for a thermopile occupying several square centimeters of skin, which is certainly out of the range of interest. Better results have been obtained in [7] that follow the earlier work [8], wherein bismuth telluride thermopiles have been fabricated on polyimide tape. Instead of waving the tape supporting the thermopile, it is cut into pieces and placed in a stack or just rolled into a Swiss roll and positioned in between circular hot and cold plates of 9.3 mm in diameter. This provides denser filling of the inner space with thermocouples, so that up to 5074 thermocouples are fabricated per button-shaped thermopile. At a height of 1.4 mm, the thermopile shows a thermal resistance of 38 K/W and generates 0.52 V and about 1 μW at a forced temperature difference of 1°C. (Note that a much lower temperature difference will build up if such thermopile is placed in contact with the skin of human being, for reasons explained below.) The advantage of a polymer carrier is in its potential flexibility and the resulting resistance of a thermopile to mechanical stresses and shocks common in wearable devices. The disadvantage is, however, the parasitic heat flow through the carrier tape despite its low thermal conductivity, because the thickness of the tape exceeds the thickness of the thermocouple layer.

Micromachined poly-Si and poly-SiGe thermopiles have been reported in [9–11]. One thermocouple occupies only 49 μm × 11 μm area, therefore, almost 16 thousand thermocouples are fabricated on a die of 3.2 mm × 2.2 mm size [11]. After release, the thermocouple microbridges are supported by thin oxide layer. The thermopile produces more than 1 V at a forced temperature difference of 1°C if recalculated to 1 cm^2 of the die filled with thermocouples. The corresponding measured power amounts, however, to about 60 nW/cm^2 for a poly-Si thermopile and about 35 nW/cm^2 for a poly-SiGe one, i.e., significantly less than for the thermopile on a polyimide tape. The reason for that is the much larger electrical resistance compared with the one of thermopiles on a polymer tape. In this sense, it was not clear in the beginning of this work whether micromachined thermopiles were able to compete on power production with both the thermopiles available on the market and polymer-tape thermopiles.

3. How to Design a Wearable Thermoelectric Generator

The problem solution departs from understanding the conditions at which the energy harvester works on the human body. The thermal circuit of a wearable TEG placed in contact with the skin involves the thermal resistance of the body and the one of ambient air. These resistors are connected in series and represent the thermal resistance of a thermal generator (Fig. 1). Despite the fact that the air is a heat sink, in terms of thermal circuit its thermal resistance acts in the same way as the one of the body (i.e., of the heat generator) and must be included into the thermal generator. (In the other words, the thermal resistance of the body and air is a thermal resistance of the environment surrounding the TEG, see [12]). The TEG represents a thermal load of this thermal generator as shown in Fig. 1. The heat flow W in the circuit can be found as the ratio of the temperature difference between the deep body temperature, or core temperature, T_{core}, and the ambient air with the temperature T_{air} to the thermal resistance of the circuit. It is obvious that the available temperature difference $\Delta T=T_{core}-T_{air}$ cannot appear on the thermoelectric generator, at least because of the high thermal resistance of ambient air. The ratio $R_{TEG}/(R_{body}+R_{air}+R_{TEG})$ determines the part of available temperature difference that is obtained on a TEG, i.e., ΔT_{TEG}, which is $T_{skin}-T_{BL}$, where T_{BL} is the temperature of a boundary convection layer. The common practice to quote the parameters of a thermopile designed for using it on human beings as per one degree of enforced and fixed temperature difference on the thermopile does not allow even approximate evaluation of actual performance of the TEGs on the skin (unless their thermal resistance and detailed embodiment are reported, which can be then used to perform the evaluation). The thermal resistors composing the thermal generator are variables and depend on each other. The air temperature is also variable, so the temperatures appearing at the boundaries of the TEG, i.e., skin temperature and the temperature of a boundary convection layer are variables, too.

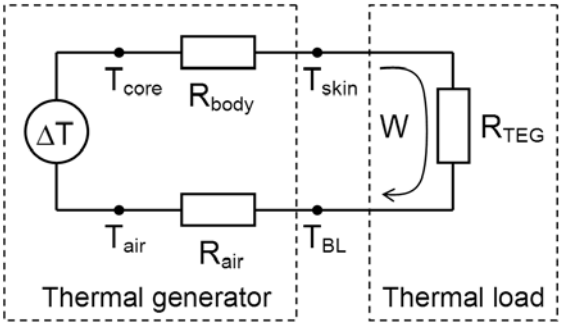

Fig. 1. Thermal circuit representing a TEG attached to human body.

In order to design a wearable TEG correctly, the knowledge of the thermal properties of human body is vitally important. It is known that metabolic activity in human beings manifests itself as a heat flow on skin of about 6 mW/cm^2 at indoor temperatures, on average [13]. However, heat transfer through conductivity, e.g., measured on a trunk of nude person standing still at a temperature difference between the skin and ambient air of 9 °C is only 3 mW/cm^2 [14]. The clothes further decrease the heat flow on covered areas, but may cause its increase in hands. About 80 % of the energy spent by a person on physical activity also turns into wasted heat however it is dissipated mostly through sweating due to the body thermoregulation. It offers only minimal increase of the conductive heat flow on skin, mostly in extremities. The mechanisms of thermoregulation of a homeotherm (warm-blooded animal) include many factors such as temperature-dependent metabolic rate, vasomotor action, panting and sweating, control of cutaneous blood flow, piloerection and shivering. These mechanisms are accomplished by behavioral thermoregulation such as choosing the cloth ensemble according to the weather (humans), wallowing in mud to increase evaporative water loss (pigs; they do not sweat), or hiding in a shadow and decreasing physical activity in a very hot day (everybody). In cold weather, the thermoregulation mainly affects the extremities while keeping the core organs within the certain temperature range. The nonuniform distribution of both muscles and subcutaneous fat over the body as well as the presence of arteries are the physical reasons for additional variation of the relevant human body properties from place to place, i.e., of (i) the heat flow density on the skin and (ii) the local thermal resistance of the body between its core (brain, liver, heart) and the skin surface in the chosen location. All above factors cause nonuniformity of skin temperature even in a nude person. The measurement of local heat flows through the skin in a wrist has been performed in [15–17]. The results show that despite comparatively small skin temperature variation around the wrist the ability of the body to produce large heat flow per square centimeter of skin varies significantly, which reflects strong variations of local thermal resistance of the body. Therefore, just by choosing the location for a TEG on a body, one can significantly enhance its performance characteristics [15].

The local heat flow from the heat source such as a human body can be further enhanced using a radiator for better heat exchange between the TEG on skin and the ambient air. The gain depends on physical size of a radiator. For technical applications, large radiators could be acceptable, while for on-body use, their size must be kept comparatively small, e.g., not exceeding the dimensions of a watch, in order not to induce discomfort to the user. Furthermore, a TEG itself can decrease the thermal resistance of the body in the location of its attachment [17] thereby further increasing the local heat flow. As it has been shown in [15], the use of a radiator is in a row of the design rules for reaching maximum power generation per unit area occupied by a TEG on the person's skin.

The plate of a TEG contacting the skin, which is called hot plate, and the radiator rejecting heat into the air represent two major outer heat-exchanging surfaces of the TEG with a thermopile between them. A large hot plate, e.g., of a watch size, and a radiator of similar size are required to obtain a heat

flow through the TEG of the order of 100–200 mW despite the fact that a micromachined thermopile die inside could be small, i.e., few millimeters in size. However, such enlargement of a TEG, especially of its radiator, decreases the thermal resistance of ambient air thereby locally increasing heat flow from the body. As a result, the heat flow exceeds the natural one and reaches about 20 mW/cm^2 in wearable devices, even in the office [16].

Above reasoning together with a requirement of 10–100 μW needed for the simplest wireless sensor nodes resulted in watch-size TEG designs, e.g., like those shown in Fig. 2 (a, b). In Fig. 2 (a), a small micromachined thermopile assembly is sandwiched in between the hot plate and the fin/pin-featured radiator. The hot plate and the sides of thermopile should preferably be thermally isolated from the air with, e.g., a layer of nanoporous material thereby ensuring that most of the heat collected by the plate is transferred directly to the thermopile and then to the radiator. A metal reflector can also help to suppress the radiation heat transfer to the radiator, while simultaneously reflecting into ambient air a part of the radiation emitted by black inner surface of radiator. A touch and shock protecting structure, e.g., a grid with high transparency for both convective heat transfer and radiation must preferably be made of thermally isolating material and/or thermally decoupled from the hot plate and skin with thermally isolating holder (in Fig. 2 (a), a polymer holder is shown). The air gap between the hot plate and radiator allows the boundary layer of convection (heated by the part of the human body located below the TEG) to pass freely in between the hot plate and the radiator. In Fig. 2 (b), a thinner TEG which is completely filled with thermal isolation (a nanoporous material, a gas with low thermal conductivity or/and at decreased pressure) is shown. Such a TEG can be only a few millimeter-thin that is advantageous for convenience of the user and for embedding such device into the clothes. The drawback is however in proximity of the cold plate, i.e., a planar radiator, to the skin, where the temperature of the air jet of free convection formed by the human body rapidly approaches the skin temperature thereby decreasing the Rayleigh number for convection on the radiator to a value less than the one on skin. Of course, all components depicted in Fig. 2 (alb) can be freely interchanged between two shown examples of TEGs. Further discussions in this article are conducted assuming that the thermopile is mounted in such TEG, so the characteristics reported below are valid only for such designs of energy harvesters and in any case cannot be obtained in a bare thermopile on the skin.

4. Micromachined Thermopiles at Limited Heat Flow

Let us discuss the simplified case of a micromachined thermopile on skin, i.e., under the condition of a heat flow limited by both body properties and the heat transfer from the radiator into the ambient air. The basic element of a thermopile is a thermocouple, composed of two legs of different thermoelectric materials, Fig. 2 (c). In order to give numerical examples we assume that the two legs are made of p- and n-type bismuth telluride-based materials with the following properties: an electrical resistivity of 10^{-5} Ω, a thermal conductivity of 2 W/m K, and a Seebeck coefficient of 200 μV/K. The legs are interconnected by metal layer forming a contact with low contact resistance to the semiconductor. In Fig. 2 (d), a thermopile composed of thousands of such thermocouples (only 16 thermocouples are depicted) is sandwiched in between hot and cold plates; the latter represents a planar radiator. The output voltage and power depend on the number of thermocouples. It can be easily shown that the maximum power is obtained when the heat flow through the thermoelectric material equals to the "parasitic" heat flow through the air located between the plates. In order to give a numerical example, let us fix the plate area to 1 cm^2 and the heat flow to 18.5 mW/cm^2. (This value is typical in a wearable TEG supplied with radiator [16].) For simplicity, we assume that the TEG operates in quiescent air at 20°C. The resistance of metal layer and the electrical contact resistance per thermocouple are assumed to be negligibly small as compared with the resistance of semiconducting legs.

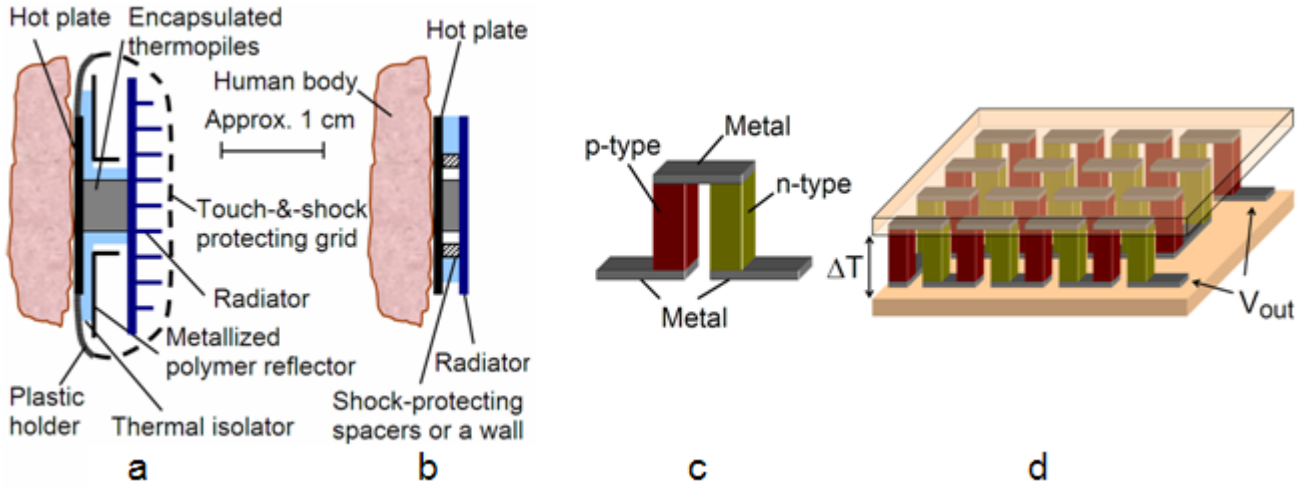

Fig. 2. The watch-thick TEG surrounded by touch- and shock-protecting grid (a) [4], the thin TEG wherein the only shock protection is provided with thermally isolating side wall or spacers (b), a thermocouple (c), and a thermopile (d). The possible scale for (a)-(b) is shown only to give an idea about the TEG size.

For calculations it is assumed that the released micromachined thermocouples are self-standing, i.e., they have no additional support, their height is 5 μm, the thickness is 0.5μm and the width is 1μm so that the effective lateral dimension, a, is $1/\sqrt{2}$ μm. In Fig. 3 (a), the output power and voltage are shown as a function of the number of thermocouples. The power is limited to only 0.11 μW, however, a large voltage, i.e., 3 V, can be obtained. The above results are very close to the measurement results reported in [11]. One can see in Fig. 3 (b) that the temperature difference on the thermopile is also low, which is confirmed in [18] for the thermopile reported in [10]. At maximum power output, the resistance of the thermopile approaches 400 MΩ that is a too high value for a generator powering electronic devices or battery chargers. The temperature difference on the thermopile at maximum power is limited to only 18 mK. The corresponding thermal resistance is 1 K/W, which is too low to obtain large temperature drop on it. One can see that the output power reaches its maximum at an optimal number of thermocouples of about 2×10^6, i.e., when the thermal resistance of the air is equal to the one of the thermopile. This large number of thermocouples can be fabricated if one thermocouple occupies a square of only 7 μm × 7 μm area, which is a difficult, but not an impossible task. The large number of thermocouples has also the obvious drawback of increased probability of getting a non-functioning device. Because the thermocouples are electrically in series, the failure of just one thermocouple would cause the failure of whole device. This drawback potentially decreases yield of good devices in the mass production and therefore affects the production cost.

The number of thermocouples, n, the temperature drop, ΔT, the output voltage, V, observed at maximum power and the maximum power itself, P_{out}, are described by the expressions:

$$n = \frac{G_{air} h}{g_{te} a^2} = \frac{A g_a}{g_{te} a^2}, \tag{1}$$

$$P_{out} = \frac{1}{16} S^2 \frac{W_u^{\,2} A^2}{g_{te} \rho} \frac{1}{G_{air}} = \frac{1}{16} S^2 \frac{W_u^{\,2} A}{g_{te} \rho} \frac{h}{g_a}, \tag{2}$$

$$\Delta T = \frac{W_u A}{2 G_{air}} = \frac{W_u h}{2 g_a}, \tag{3}$$

$$V = \frac{W_u A S}{2 g_{te}} \frac{h}{a^2}, \tag{4}$$

where A is the area of the hot/cold plate, a and h are the lateral size and the height of legs, respectively, g_a is the thermal conductivity of air, g_{te} is the thermal conductivity of thermoelectric material, ρ is its resistivity, S is Seebeck coefficient, G_{air} (which is equal to $g_a A/h$) is the thermal conductance of the air between the plates, and W_u is heat flow per unit area. One can spot that the number of thermocouples required for reaching the power maximum does not depend on their height. The temperature difference and the generated power are inversely proportional to the thermal conductance of the air between plates. The latter is large in micromachined thermopiles at a height of a few micrometers therefore the temperature drop and the power are both low in these devices. The output voltage depends on the ratio h/a^2 that for the chosen geometry of micromachined thermopiles corresponds to the best thermopiles available on the market nowadays. Equations (1)–(4) suggest that increasing the height h is beneficial in terms of output power. However, the aspect ratio, h/a, is typically technology-limited. If both these quantities, h and a, are increased by a factor of q the power is multiplied by q and the voltage is divided by q, but in order to power electronics effectively the voltage cannot drop below a certain limit. This consideration shows that there is a need of a different design wherein voltage and power can be controlled independently. The design of such a thermopile is the core of this section.

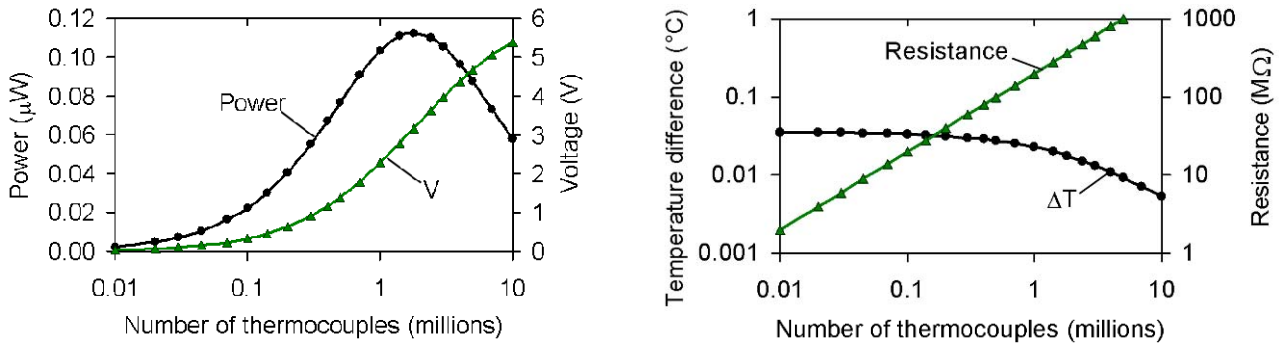

(a) (b)

Fig. 3. (a) Dependence of the voltage and power in the matched load on number of thermocouples calculated for a micromachined thermopile placed in between the hot and cold plates of 1cm^2 area each. (b) Dependence of the resistance and temperature drop over a micromachined thermopile on number of thermocouples at an available temperature difference of 10 °C between the hot plate and ambient air.

Let us analyze another micromachined thermopile, which we are going to build using the basic element shown in Fig. 4 (a). It represents a pillar made of the material with high thermal conductivity, namely, silicon. Its height, $(H–h)$, is about 1.5 mm, while the lateral size b is of the order of 10 μm. The pillar is cut in two parts in the middle and a micromachined thermocouple with a lateral size a of the order of 1 μm and a height h of the order of several micrometers is sandwiched in between the two parts of the pillar. We will now insert an increasing number of these basic elements in between the plates of the same size as in previous example. This is equivalent to an increase of the die size proportional to the number thermocouples as shown in Fig. 4 (b). Hereafter, we will call this die the thermopile assembly because in production, the two sets of semi-pillars correspond to two standard silicon wafers with a thermopile sandwiched in between. Fig. 4 (b) suggests that in such thermopile the parasitic thermal conductance of air in between two plates is mainly controlled by H, and is very low, while the output voltage of the thermocouple is controlled by the ratio h/a^2, which is, as desired, large. The performance of such thermopile can be described by the following equations:

$$n = \frac{G'_{air} h}{g_a b^2 + g_{tc} a^2}, \tag{5}$$

$$P_{out} = \frac{1}{16} S^2 \frac{W_u{}^2 A^2}{\rho} \frac{1}{G'_{air}} \left(g_{te} + \frac{b^2}{a^2} g_a \right)^{-1}, \tag{6}$$

$$V = S \frac{WA}{2} \frac{h}{g_a b^2 + g_{te} a^2}, \tag{7}$$

where G'_{air} is equal to $g_a A/H$. In order to compare these expressions with the ones obtained for the micromachined thermopile of Fig. 2 (d), namely, expressions (1), (2) and (4), one should notice that typically g_a is of the order of 100 times less than g_{te}. This means that until b is smaller than 10 a, the term $g_a b^2$ is smaller than the term $g_{te} a^2$. As a consequence, approximating $(g_a b^2 + g_{te} a^2)$ with $g_{te} a^2$ will result in an error of at most a factor of two. With this in mind, we notice that Eq. (5) for the maximum number of thermocouples and Eq. (6) for the power are the same as Eqs. (1) and (2), but now G'_{air} is small. As a consequence, the number of thermocouples required to obtain the maximum power is dramatically reduced, while the maximum power itself is increased. Eq. (7) is also similar to Eq. (4). The voltage depends mainly on the dimensions of thermocouples, i.e., on the term h/a^2, therefore the output voltage is large, as desired.

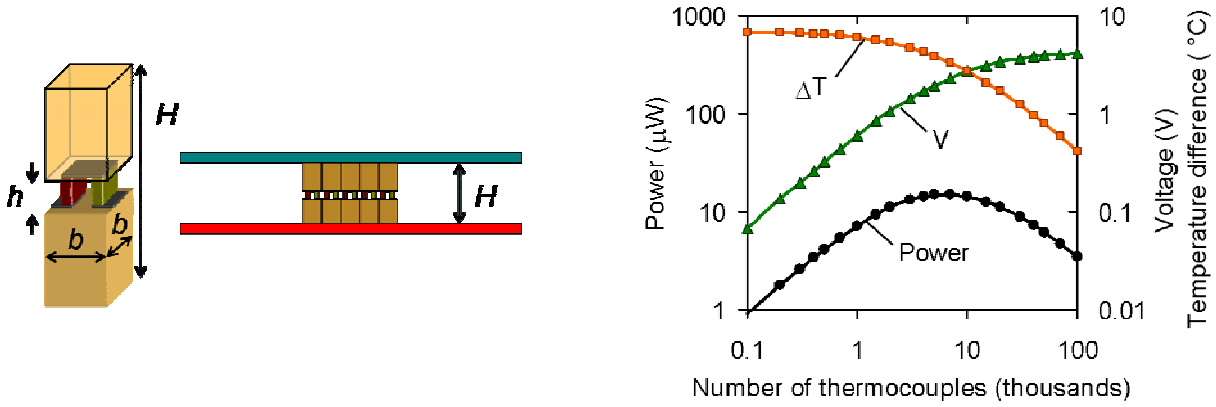

(a) (b) (c)

Fig. 4. (a) Basic thermocouple element consisting of a thermocouple sandwiched in between two dies, (b) the thermopile composed from variable number of such basic elements placed in between the plates, and (c) dependence of the voltage and the power on the matched load calculated for such thermopile on a pillar in between the plates of 1 cm^2 each. Also shown is the temperature difference on the thermopile at the same available temperature difference of 10°C between the hot plate and ambient air, as before, in Fig. 3.

Fig. 4 (c) shows the dependence of power and voltage on the number of thermocouples. (In the calculations, H=1.5 mm, b=5 μm, h=5 μm and a=0.7 μm have been used.) At a maximum power of 15 μW, which is more than 100 times larger than the one obtained in Fig. 3 (a), the voltage is 2.3 V, i.e. only slightly less, despite the fact that the number of thermocouples is decreased by a factor of about 300. Fig. 4 (c) also illustrates the obtained temperature difference ΔT, which now reaches several degrees Celsius when the number of thermocouples n is small. At an optimal value of n=7000,

it equals to 3.3 °C. An additional advantage is that by using a drastically reduced number of thermocouples the resistance decreases by a factor of 300 and the yield problems are much less severe. It is evident that the micromachined thermopile supplied with a pillar would provide a TEG featuring a large voltage and a large power at the same time. Below we will discuss how a structure like the one of Fig. 4 (b) can be fabricated, and we will evaluate its performance characteristics taking into account technology limitations. The next section is dedicated to the description and modeling of a thermocouple. A thermopile composed from such thermocouples is discussed afterwards.

5. Finite Element Modeling of a Single Thermocouple

Two materials, i.e., BiTe and poly-SiGe have been considered in this work for the fabrication of micromachined thermopiles. BiTe provides better performance characteristics while poly-SiGe offers a greater ease of fabrication, as it is a commonly used material in the microelectronic industry. In this section, the case of poly-SiGe is modeled in detail and used to identify the effects of various parameters on performances. Effects are qualitatively the same in case of BiTe. The structure of a poly-SiGe thermocouple designed for fabrication of thermopiles is shown in Fig. 5. Narrow poly-SiGe legs are interconnected at wider top and bottom junctions by aluminum pads. The microelectronic processes are almost planar and allow only a minor topography, while a topography of 5–10 μm is needed for reaching good performance characteristics. Therefore a design where the total topography is shared between the substrate and the thermocouple has been adopted. A 2.5 μm-deep trench is etched in the silicon substrate under the cold junction to obtain a 5 μm separation from the substrate, while keeping the topography below 3 μm. However, as it is difficult to reproduce even such topography at 1–2 μm resolution required for the legs, the thermocouple was modeled at the step height h from 0.5 to 3 μm, as shown in Fig. 5. The width of thermocouple legs ($w2$) is reduced to the limit of contact lithography (1 to 3 μm is used in different designs) to increase their thermal resistance. The junction zones are made wider, 3–10 μm, ($w1$ in Fig. 5) to provide low contact resistance between poly-SiGe and aluminum. The size of the basic thermocouple element varies depending on $w1$, for instance, the thermocouple shown in Fig. 5 occupies an area of 30 μm × 16 μm on the die.

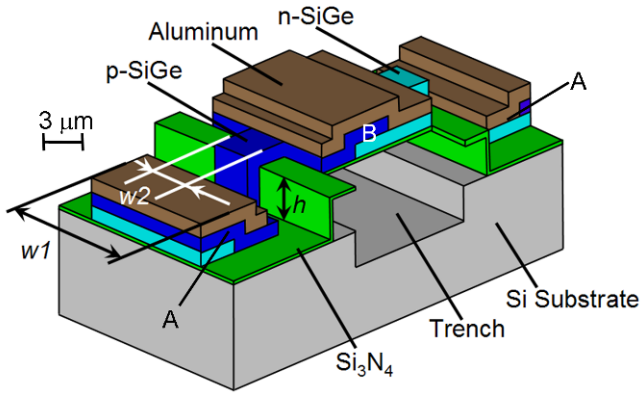

Fig. 5. The schematic of a thermocouple representing a self-supported microbridge over the trench with up to 3 μm-high step h between hot (A) and cold (B) junctions.

The behavior of the thermocouple has been analyzed using FEM. A fully 3D model of the thermocouple in thermal contact with the top die (through 0.5 μm-thin indium solder layer on cold junctions) has been built in the software MSC Marc according to the real dimensions, as shown in Fig. 6. The model is composed from 2.6×10^4 elements and 3.1×10^4 nodes. The properties of the materials used in the model have been obtained in our experiments or taken from the literature. For the

examples of simulations shown in this section, the height h and width $w2$ of thermocouple legs are fixed at 3 μm. Two parameters at the level of a thermocouple have been obtained from FEM. The first one is the thermal resistance of thermocouple element including the two dies, the air in between them, and the thermocouple itself. This thermal resistance was then used at the level of a TEG to calculate sequentially the heat flow and temperature difference between the top and bottom of the basic thermocouple element shown in Fig. 6 (a). The temperature difference between the thermocouple junctions, which actually determines the generated power, is smaller. Consequently, the second parameter obtained in FEM is the ratio of the temperature difference in between the thermocouple junctions to the one across the basic thermocouple element.

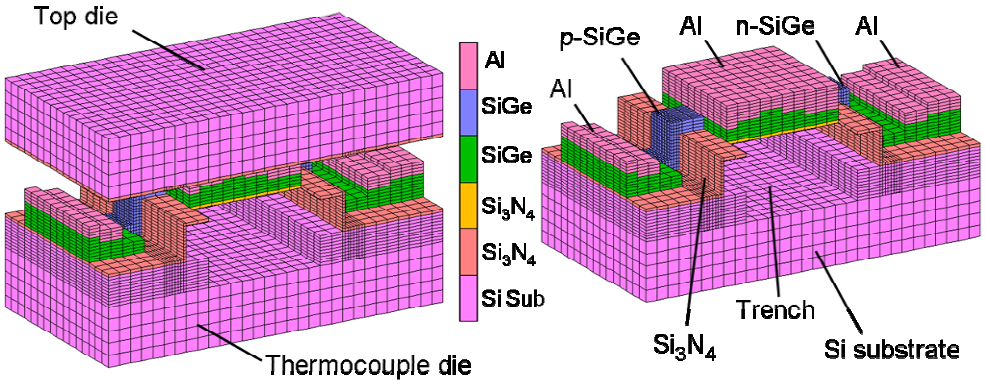

(a) (b)

Fig. 6. The 3D mesh in the finite element model of the basic thermocouple element with a thermocouple die covered with a top die (a), and of the bottom die with a thermocouple (b).

The thermal resistance of a single thermocouple can be determined from FEM simulation through supplying a known heat flow into the bottom surface, while the temperature at top surface is fixed. Doing so, the temperature difference between the two surfaces can be found. The thermal resistance is then calculated as the ratio of temperature difference to heat flow. The actual fabrication process, described in detail elsewhere [19] includes deposition of a sacrificial SiO_2 in the trench. The former is removed afterwards at the last step of manufacturing, so the thermopile is released. Fig. 7 shows the temperature distribution in a thermocouple before and after release. The temperature difference observed on the parts of thermocouple legs not coated with interconnecting metal significantly increases after release as seen in Fig. 7 (b). The heat flow applied in this simulation is 100 mW/mm^2 that corresponds to a heat flow of 48 μW through the thermocouple element and results in a thermal resistance of 2.4×10^4 K/W before release and of 1.25×10^5 K/W after release. Modeling shows that decreasing the height h to 0.5 μm causes decreasing of the thermal resistance by a coefficient of two, to 6.1×10^4 K/W.

The second important parameter extracted from FEM is the percentage of the total temperature difference appearing between the thermocouple junctions. The calculated relative temperature variation in the poly-SiGe layer is shown in Fig. 8 (a). The data refer to the case of released thermocouple. It can be seen that the temperature difference between the two thermocouple junctions reaches 57% of the one applied to the element. It is worth mentioning that before release, it is only 37%. Of course, some further improvements of the design can be done, e.g., no overlapping of two poly-SiGe layers on hot junctions can increase their distance to the cold die. The top die can also feature trenches similar to those in thermopile die, located over the cold junctions, thereby further increasing the thickness of an air gap, improving both the efficiency of using the temperature difference and, as a consequence, the thermocouple performance characteristics. However, the target

of this simulation was to model the performance of the thermopiles supposed to be fabricated as a proof of the concept therefore no further changes to the design have been implemented.

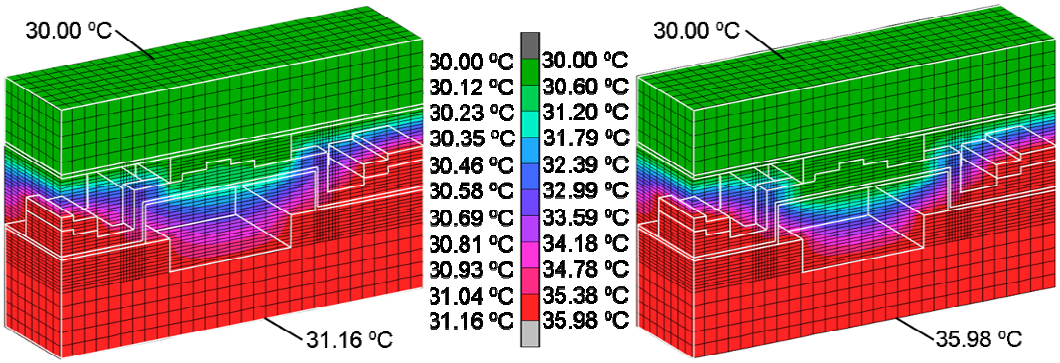

(a) (b)

Fig. 7. Simulated temperature distribution in the middle (cross section) of the thermocouple element with 3 μm topography at the boundary conditions of fixed heat flow and fixed temperature at the top surface: (a) before release, and (b) after release.

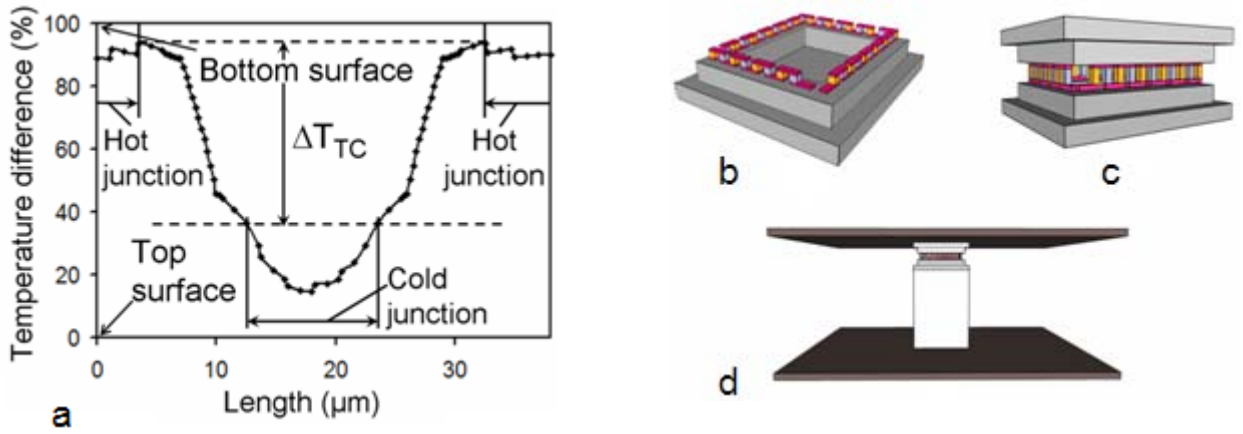

Fig. 8. (a) Relative temperature difference with the cold surface along the thermocouple at fixed temperatures of top and bottom of the thermocouple element shown in Fig. 6a, (b-c) Schematics of the thermopile die with a thermopile on a rim (b), of the thermopile die capped with a top cold die also featuring a rim (c), and of the complete assembly (d).

6. Modeling of the Thermoelectric Generator

Due to the complexity of the structure, a finite element model cannot be created for a thermoelectric generator. Instead, an analytical model was built, which consider an assembly of thousand of thermocouples connected thermally in parallel and electrically in series. The thermal resistance derived from FEM for a thermocouple is used in the model. As in the previous section, we discuss the case of poly-SiGe-based devices for understanding the behavior of the thermopile. Results for BiTe are briefly given at the end of the section.

Poly-SiGe thermopiles made of 2500 or 5000 thermocouples have been modeled. Depending on the number of thermocouples and their size, the thermopile occupies an area of 0.6 to 2.3 mm^2. Such small size of the die would complicate its assembling with the cold die on a die-to-die basis. In order to

alleviate this problem we have placed the thermopile on a 4 mm × 5 mm die. However, the air in a 1–3 μm gap between such two dies would thermally shunt the thermopiles thereby dramatically decreasing the temperature difference between the thermocouple junctions. To avoid this problem, the die is thinned down everywhere except the zone covered with thermocouples, thereby making a 250 μm-tall square rim under the thermopile, see Fig. 8 (b). The top cold die to be assembled with the thermopile die by flip-chip bonding, also features a rim; the assembly is shown in Fig. 8 (c). As a result, the mean distance between the thermopile die and the cold one increases in about 1000 times due to the rim. Calculations show that if the assembly shown in Fig. 8 (c) is placed between two watch size plates, the parasitic air conductance between them is still too high and adversely affects the performance characteristics of the thermopile. Therefore, a distance of several millimeters is required between the plates in this particular case, so non-standard thick silicon wafers would be necessary. The simpler solution found in [15] is applied instead, i.e., the thermopile assembly is placed on a 6 mm-tall pillar, thereby a distance H of 8 mm in between the plates is provided despite using standard silicon wafers. Assuming the both plates of 1mm-thick, the thickness of the TEG becomes 1cm. The final assembly shown in Fig. 8 (d) is the one used for the modeling below.

The equivalent circuit for analytical modeling is shown in Fig. 9. It is composed of thermal resistors corresponding to different components of the TEG and of the environment. The thermopile, in turn, represents n basic thermocouple elements modeled in previous section. As shown in Fig. 8 (b), the thermocouples are connected thermally in parallel and electrically in series, like in Fig. 2 (d). In the equivalent circuit, according to electro-thermal analogy, the temperature difference, the thermal resistance and the heat flow in thermal domain are replaced with the voltage, the electrical resistance and the current in electrical domain, respectively. A core temperature of the human body of 37 °C is assumed, while the temperature of the ambient air is set to a typical one, i.e., 22 °C. The human body and ambient air (the latter is represented by the resistors corresponding to convection and radiation) are necessary components of the circuit, according to Fig. 1. Due to the fact that the thermopile and the top die are etched to form the two rims, a corresponding air gap resistor, "Air, d-d", appears in between the dies as shown in Fig. 9.

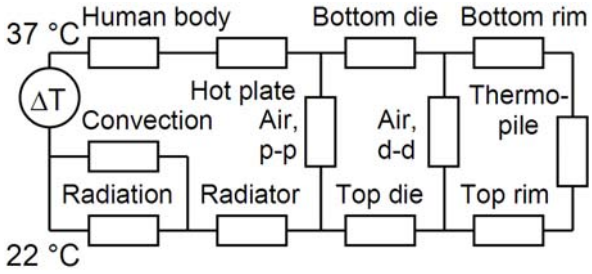

Fig. 9. Equivalent thermal circuit for analytical modeling of the TEG, where 'd-d' and 'p-p' denote the heat exchange through the air between two dies and two plates, respectively.

The voltage and the power transferred from the TEG, Fig. 8 (d), into a matched load as a function of the number of thermocouples is shown in Fig. 10. For comparison, the characteristics of the thermopile with no rim in silicon die are also plotted confirming importance of this design element. For the shown example of a thermocouple element, Fig. 8, and at the chosen both temperature of the ambient air and thickness of the TEG (1 cm), the output power of 1.6μW maximizes at 2100 thermocouples. The corresponding voltage on the matched load of 0.75 V is provided thereby allowing its efficient step-up conversion for powering wearable devices. Calculations show that depending on the type of thermocouples and their number, the power and voltage on the matched load are 0.2–1.6 μW and 0.25–0.75 V, respectively. These values indicate typical characteristics of discussed micromachined thermopiles in wearable devices. Replacement of poly-SiGe with BiTe would allow reaching 8 μW

and 1.1 V in a similar device at a state-of-the-art thermoelectric figure-of-merit ZT of 0.9. Furthermore, if higher topography is provided (i.e., with taller thermocouples), the power generated by micromachined thermopiles could approach the power obtained in wearable TEGs with commercial thermocouples [20], i.e., 25–30 μW/cm^2, but with better output voltage, smaller size and much lower production cost. These characteristics can be obtained in a 1.5 cm-thick TEG. In thinner versions, neither with micromachined, nor with commercial thermopiles this limit of power generation on open skin cannot be reached at specified conditions, on 24-hour average. For example, the maximum of power shown in Fig. 10 for a thermopile on a rim decreases to 0.85 μW in a 4 mm-thick TEG.

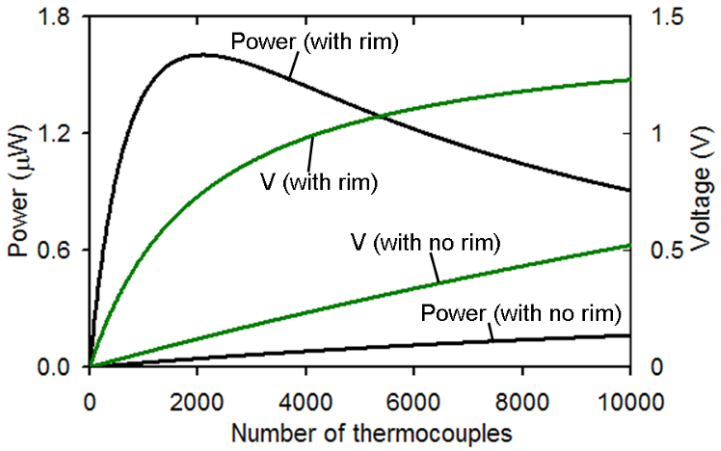

Fig. 10. Simulated voltage and power generated by a watch-size TEG depicted in Fig. 8 (b-d) containing a variable total number of the thermocouples shown in Fig. 5.

7. Conclusions

Effective thermal arrangement of the thermoelectric generator for wearable devices is discussed which increases the heat flow from the wearer through the generator well above the natural heat flow through the skin. The design of a micromachined thermopile specially suited for energy harvesting on "difficult" heat sources like human beings is described. It solves the problem of parasitic heat flow inside the device known as a key factor deteriorating the performance of micromachined thermopiles as compared with large-size ones available on the market. In addition, utilization of a thermally conducting pillar (or, generally speaking, a thermal shunt [21]) located thermally in series with the thermopile allows redirection of the heat flow inside the TEG into the thermopile. The pillar decreases the heat flow flowing directly from hot plate to a cold plate through the air inside the device and forces it to flow through the thermopile instead. For a practical embodiment and proof of the concept, a poly-SiGe thermopile suited for contact photolithographic process flow has been modeled offering a voltage up to 0.75 V and the power of 1.6 μW in a 3 cm × 3 cm × 1 cm TEG. The power is still small, but it is already several orders of magnitude higher than in existing micromachined TEGs if placed on the human body. The results of this work have been used for developing the technological process and fabrication of micromachined thermopiles and a wrist TEG with such thermopile [19]. The reported experimental results confirm the ideas presented in this paper. According to the modeling of wearable thermopiles at indoor conditions, the MEMS-based watch-size TEGs of the future could produce, depending on materials of thermopiles, from about 20 μW with poly-SiGe to 100–150 μW with BiTe at the voltage exceeding 1V. However, to reach this target, the height of thermocouples must be dramatically increased up to 10–15 μm while keeping a small feature size of 2–3 μm. The related research has already started using a projection photolithography at low numerical aperture and the height of 6 μm has been already reached [16, 22]. In case of success, wearable TEGs with micromachined thermopiles are expected to outperform solar cells on energy production on human

beings, on 24-hour average, in moderate climate, because the performance and efficiency of solar cells are affected by typical lack of illumination in the buildings while thermoelectric converters effectively work day and night. In nearest future, the polycrystalline SiGe is to be replaced with better thermoelectric material, e.g., BiTe. The basic principles and way of designing wearable thermoelectric energy harvesters discussed in this paper are very general and therefore can be applied to any other application of thermoelectric generators for energy harvesting.

Development of low-cost micromachined thermopiles in coming years certainly could move the balance of the market preferences in favor of body-powered devices with no need in primary batteries, so that mass production of such wearable devices would be beneficial. In particular, this is related to limited resources on our planet, namely, to the limited annual production of thermoelectric materials. Indeed, a micromachined thermopile contains about 10^{-6} of thermoelectric material that is required in the smallest thermopiles on the market while theoretically offering about the same power produced in energy harvesters. Therefore, the only one gram of thermoelectric materials is sufficient for fabrication of millions devices. The fabrication cost in mass production is expected to be lower than the cost of its closest and strongest competitor, namely, lithium batteries. Furthermore, such miniature thermopiles, if used in implantable devices, can trigger the development of a huge variety of implants featuring a completely safe energy supply for the entire lifetime of a patient.

Acknowledgements

This work has been performed in 2003–2007 within the internal Human++ program. The authors are grateful to J. De Boeck, B. Gyselinckx and R. J. M. Vullers (Holst Centre/IMEC-NL, Eindhoven, The Netherlands) for providing continuous encouragement and motivation.

References

[1]. http://www.xs4all.nl/~doensen/p.html

[2]. M. Kishi, H. Nemoto, T. Hamao, M. Yamamoto, S. Sudou, M. Mandai, S. Yamamoto, Micro-thermoelectric modules and their application to wristwatches as an energy source, in *Proc.of 18th Int. Conf. on Thermoelectrics (ICT'99)*, Baltimore, MD, 29 August-2 September 1999, pp. 301-307.

[3]. T. Torfs, S. Sanders, C. Winters, S. Brebels, C. Van Hoof, Wireless network of autonomous environmental sensors, in *Proc.of IEEE Int. Conf. on Sensors*, Vienna, Austria, 24-27 October 2004, Vol. 2, pp. 923-926.

[4]. T. Torfs, V. Leonov, R. J. M. Vullers, Pulse oximeter fully powered by human body heat, *Sensors & Transducers,* 80, 6, 2007, pp. 1230-1238, http://www.sensorsportal.com/HTML/DIGEST/P_151.htm

[5]. S. Hasebe, J. Ogawa, M. Shiozaki, T. Toriyama, S. Sugiyama, H. Ueno, K. Itoigawa, Polymer based smart flexible thermopile for power generation, in *Proc.of 17th IEEE Int. Conf. Micro Electro Mech. Sys. (MEMS)*, Maastricht, The Netherlands, 25-29 January 2004, pp. 689-692.

[6]. S. Hasebe, J. Ogawa, M. Shiozaki, T. Toriyama, S. Sugiyama, H. Ueno, K. Itoigawa, Fabrication of flexible thermopile generator, *J. Micromech. Microeng.,* 15, 2005, pp. S233-S238.

[7]. I. Stark, Thermal energy harvesting with Thermo Life®, in *Proc. of Int. Workshop Wearable and Implantable Body Sensor Networks (BSN'06)*, Boston, MA, 3-5 April 2006, IEEE DOI 10.1109/BSN.2006.37.

[8]. I. Stark, M. Stordeur, New micro thermoelectric devices based on bismuth telluride-type thin solid films, in *Proc. of 18th Int. Conf. on Thermoelectrics (ICT'99)*, Baltimore, MD, 29 August-2 September 1999, pp. 465-472.

[9]. M. Strasser, R. Aigner, G. Wachutka, Analysis of a CMOS low power thermoelectric generator, In *Proc. 14th Eur. Conf. Solid-State Transducers (EUROSENSORS XIV)*, Copenhagen, Denmark, 27-30 August 2000, pp. 17-20.

[10]. M. Strasser, R. Aigner, M. Franosch, G. Wachutka, Miniaturized thermoelectric generators based on poly-Si and poly-SiGe surface micromachining, *Sensors and Actuators A,* 97–98, 2002, pp. 535-542.

[11]. M. Strasser, R. Aigner, C. Lauterbach, T. Sturm, M. Franosch, G. Wachutka, Micromachined CMOS

thermoelectric generators as on-chip power supply, In *Proc. 12th Int. Conf. Solid-State Sensors, Actuators and Microsystems (Transducers'03)*, Boston, MA, 8-12 June 2003, pp. 45-48.
[12]. V. Leonov, P. Fiorini, Thermal matching of a thermoelectric energy scavenger with the ambience, in *Proc. of 5th European Conf. on Thermoelectrics (ECT)*, Odessa, Ukraine, 10-12 September 2007, pp. 129-133.
[13]. J. Monteith, L. Mount, Eds., Heat loss from animals and man, *Butterworths,* London, 1974.
[14]. U. Danielsson, Influence of activity and wind on the local convective heat and mass transfer from nude man, in *Proc. of 4th Int. Conf. on Environmental Ergonomics (ICEE)*, Austin, TX, September 1990, pp. 535-542.
[15]. V. Leonov, T. Torfs, P. Fiorini, C. Van Hoof, Thermoelectric converters of human warmth for self-powered wireless sensor nodes, *IEEE Sensors J.,* 7, 5, 2007, pp. 650-657.
[16]. V. Leonov, Z. Wang, R. Pellens, C. Gui, R. Vullers, J. Su, Simulations of a non-planar lithography and of performance characteristics of arcade microthermopiles for energy scavenging, in *Proc. of 5th Int. Energy Conversion Engineering Conf. (IECEC)*, St. Louis, MO, 25-27 June 2007, DOI: AIAA-2007-4782.
[17]. V. Leonov, R. J. M. Vullers, Thermoelectric generators on living beings, in *Proc.of 5th European Conf. on Thermoelectrics (ECT)*, Odessa, Ukraine, 10-12 September 2007, pp. 47-52.
[18]. H. Böttner, Thermoelectric Micro Devices: current state, recent developments and future aspects for technological progress and applications, in *Proc. of 21st Int. Conf. on Thermoelectrics (ICT)*, Long Beach, CA, 25-29 August 2002, pp. 511-518.
[19]. Z. Wang, V. Leonov, P. Fiorini, C. Van Hoof, Realization of a poly-SiGe based micromachined thermoelectric generator for human body applications, *Sensors and Actuators A*, 2009, in press.
[20]. M. Van Bavel, V. Leonov, R. F. Yazicioglu, T. Torfs, C. Van Hoof, N. E. Posthuma, R. J. M. Vullers, Wearable battery-free wireless 2-channel EEG systems powered by energy scavengers, *Sensors & Transducers,* 94, 7, 2008, pp. 103-115, http://www.sensorsportal.com/HTML/DIGEST/P_300.htm
[21]. V. Leonov, Thermal shunts in thermoelectric energy scavengers, *J. of Electronic Materials*, 2009, in press.
[22]. J. Su, R. J. M. Vullers, M. Goedbloed, Y. van Andel, V. Leonov, Z. Wang, Process development on large-topography microstructures for thermoelectric energy harvesters, in *Proc. of 3rd Eur. Conf. Smart Systems Integration*, Brussels, Belgium, 10-11 March 2009. VDE VERLAG GMBH: Berlin, T. Gessner, Ed., in press.

Guide for Contributors

Aims and Scope

Sensors & Transducers Journal (ISSN 1726-5479) provides an advanced forum for the science and technology of physical, chemical sensors and biosensors. It publishes state-of-the-art reviews, regular research and application specific papers, short notes, letters to Editor and sensors related books reviews as well as academic, practical and commercial information of interest to its readership. Because it is an open access, peer review international journal, papers rapidly published in *Sensors & Transducers Journal* will receive a very high publicity. The journal is published monthly as twelve issues per annual by International Frequency Association (IFSA). In additional, some special sponsored and conference issues published annually. *Sensors & Transducers Journal* is indexed and abstracted very quickly by Chemical Abstracts, IndexCopernicus Journals Master List, Open J-Gate, Google Scholar, etc.

Topics Covered

Contributions are invited on all aspects of research, development and application of the science and technology of sensors, transducers and sensor instrumentations. Topics include, but are not restricted to:

- Physical, chemical and biosensors;
- Digital, frequency, period, duty-cycle, time interval, PWM, pulse number output sensors and transducers;
- Theory, principles, effects, design, standardization and modeling;
- Smart sensors and systems;
- Sensor instrumentation;
- Virtual instruments;
- Sensors interfaces, buses and networks;
- Signal processing;
- Frequency (period, duty-cycle)-to-digital converters, ADC;
- Technologies and materials;
- Nanosensors;
- Microsystems;
- Applications.

Submission of papers

Articles should be written in English. Authors are invited to submit by e-mail editor@sensorsportal.com 8-14 pages article (including abstract, illustrations (color or grayscale), photos and references) in both: MS Word (doc) and Acrobat (pdf) formats. Detailed preparation instructions, paper example and template of manuscript are available from the journal's webpage: http://www.sensorsportal.com/HTML/DIGEST/Submition.htm Authors must follow the instructions strictly when submitting their manuscripts.

Advertising Information

Advertising orders and enquires may be sent to sales@sensorsportal.com Please download also our media kit: http://www.sensorsportal.com/DOWNLOADS/Media_Kit_2009.pdf

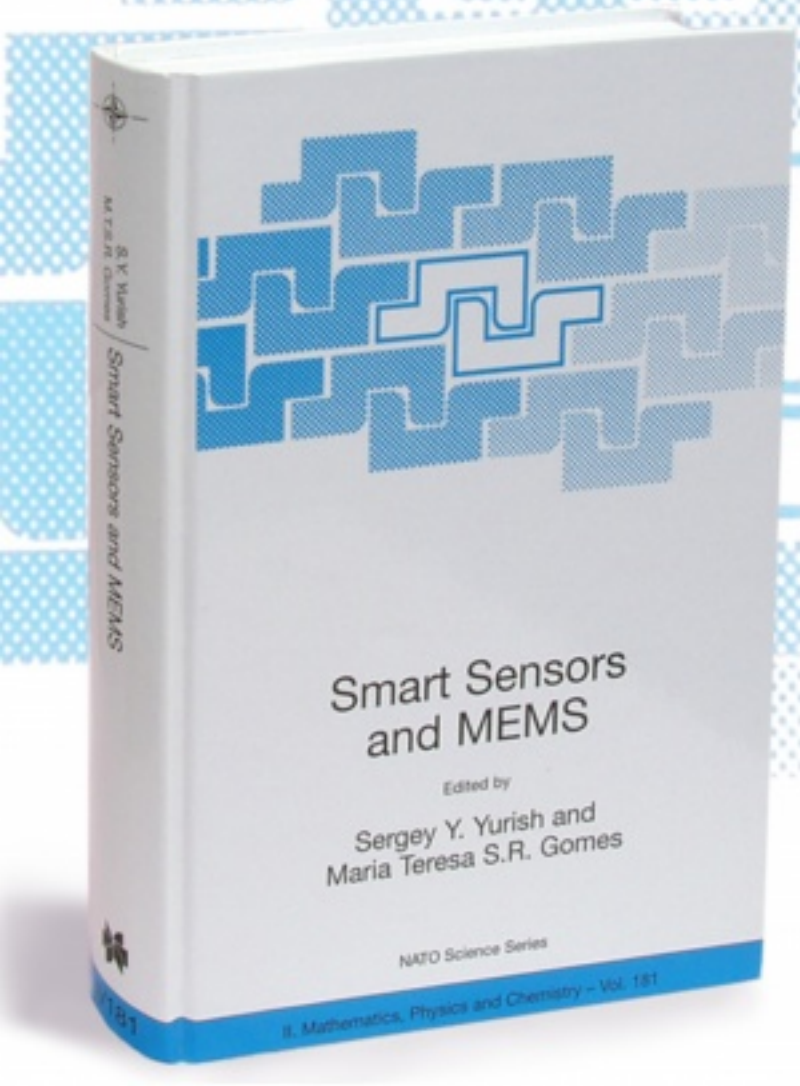

Smart Sensors and MEMS

Edited by

Sergey Y. Yurish and
Maria Teresa S.R. Gomes

The book provides an unique collection of contributions on latest achievements in sensors area and technologies that have made by eleven internationally recognized leading experts ...and gives an excellent opportunity to provide a systematic, in-depth treatment of the new and rapidly developing field of smart sensors and MEMS.

The volume is an excellent guide for practicing engineers, researchers and students interested in this crucial aspect of actual smart sensor design.

Kluwer Academic Publishers